RSC Advances

ROYAL SOCIETY OF CHEMISTRY

www.rsc.org/advances

Cite this: DOI: 10.1039/c0xx00000x

www.rsc.org/xxxxxx

ARTICLE TYPE

Nucleation and growth orientation of zinc electrocrystallization in the presence of gelatin in Zn(II)-NH_3-NH_4Cl-H_2O electrolytes

Zhimei Xia,[a,b] Shenghai Yang,*[a] and MoTang Tang,[a]

Received (in XXX, XXX) Xth XXXXXXXXX 20XX, Accepted Xth XXXXXXXXX 20XX

DOI: 10.1039/b000000x

Nucleation and growth orientation of zinc electrodeposition in Zn(II)-NH_3-NH_4Cl-H_2O solutions were studied. XRD and SEM were used to characterize the structure and morphology of deposited-Zn film on cathode. TEM and HRTEM were used to characterize the structure of zinc nuclei electrodeposited on a copper grid directly. Cyclic voltammetry was applied to investigate nucleation process of zinc crystal. The growth orientation was assessed using Lotgering factor *f* according to peaks of XRD patterns. The results showed that the additive of gelatin played a role of controlling {110} orientation of zinc crystal with maximum Lotgering factor *f* of 0.71 during zinc deposition. Change of overpotential, difference in stripping potential of different crystal orientation, controllable shape and size of zinc nuclei were observed with increase of the content of gelatin. Shape of zinc nuclei was changed from fiber to particles when the content of gelatin was 75 mg/L in solution.

1 Introduction

Zinc is a very important metal widely used in the manufactured products such as galvanized pipe, batteries, zinc alloy etc. Zinc metal is mainly produced by electrodeposition in parallel plate electrolytic cells from aqueous solutions containing zinc sulfate (Zn^{2+} 40 to 60 g/L) and sulfuric acid (H_2SO_4 150 to 200 g/L) under current densities ranging from 400 to 650 A/m^2 at 45°C or so. These ranges of operating conditions in sulfuric acid system have been determined through years of trial and error using conventional solution purification techniques. The zinc-bearing materials are usually submitted to a thermal treatment[1]in which zinc is vaporized and deoxidized from crude zinc oxide containing quite high concentrations of heavy metals and halides. Additionally, many other zinc-containing materials such as second zinc oxide from the slag of lead smelting also contain high concentration of chloride and fluoride. In any case, before being fed to the leaching process, the crude zinc oxide has to be treated to eliminate or reduce the content of halides which are noxious to the electrodepositing process. For example, chlorides and fluorides fed in the zinc sulphate electrolyte lead to chlorine evolution on anode causing labor health problems and increasing the anodic corrosion rate, compromising the zinc quality. The fluorides, even at very low concentration, heavily compromise the cathode stripping.

At the beginning of nineties, Engitec developed firstly the EZINEX process to prepare metallic zinc directly from crude zinc oxide through treating with a concentrated NH_4Cl solution at temperature higher than 80℃.[2] The similar hydrometallurgical process was used to treat low-grade oxides ores in NH_3-NH_4Cl-H_2O solution. The thermodynamics, leaching kinetics and cathodic reaction mechanism of Zn(II)-NH_3-NH_4Cl-H_2O system were studied as well. The dependence of multiple Zn(II) complexes on pH, $NH_3 \cdot H_2O$ concentration, Zn^{2+} concentration and foreign ions concentration was obtained.[3-8]

Traditionally, various kinds of leveling agents including proteinous additives and tetra-alkyl ammonium chlorides have already been found to be effective in producing dense metal coatings. Gelatin was also used in acidic H_2SO_4 and HCl electrodeposition system to obtain smooth and compact Zn film and inhibit depolarization of cathode.[9-12] Gelatin was found to improve the current efficiency and flatness of zinc deposits especially in the presence of a mixture of foreign cations.[13] The similar results were reported when gelatin was used in copper bio-metallurgical process.[14] Gelatin also helped leveling the cathodic metal surface owing to increasing the local electric resistivity in front of the dendrite and favoring growth of metal on the slack areas of the cathode.[15]

Nucleation and crystal growth played an important role during zinc electrocrystallisation and became more and more attractive interest in wet chemical eletrometallurgy of zinc. Addition of organic additives or surfactants in zinc eletrolyte not only help increasing current efficiency, smoothness of zinc deposits and decrease of acidic mist generation, but also change the growth orientation of zinc crystal in acidic sulphate solution and nucleation mechanism. The preferred orientation was reported in the presence of triethylbenzylammonium chloride, thiourea, organic colloids, polyethoxylated additives and aliphatic chain in arenes.[16-19] D. Dhak and Mackinnon et al also reported the influence of Saponin and Tennafroth 250 on preferable orientation in (101), (102), (103) and (112) planes during zinc eletrowinning in sulphate system.[20,21] Alvarez and Salinas reported that addition of gelatin caused variation of instantaneous

nucleation in sulphate electrolyte without additives.[22] Additionally, nucleation mechanism was also controlled by overpotential, magnetic field, concentration of electroactive sites and temperature in acidic electrolyte.[23-24]

However, the effects of gelatin on electrochemical nucleation and zinc crystal growth were seldom investigated now in ammonia-ammonium chloride solution (NH_3-NH_4Cl-H_2O). The aims of this work were to investigate the effects of gelatin on the formation of zinc nuclei and orientation growth on cathode in NH_3-NH_4Cl-H_2O system using TEM, cyclic voltammetry in conjunction with XRD.

2 Experiments and characterization

Electrolyte solutions(0.5mol/L of Zn^{2+}, 5.0mol/L of NH_4Cl and 1.8 mol/L of $NH_3 \cdot H_2O$) were made from the reaction of ZnO, NH_4Cl and $NH_3 \cdot H_2O$ with 28 wt% NH_3 in water (Analytical grade, Shanghai Chemistry Reagent Company, China). The gelatin was added into electrolyte when zinc electrodepositing was carried out.

Within an electrolysis cell, a copper grid was stuck on Ti-cathode and then electrodeposition was performed at current 0.02A for 3s (Shown in Fig.1). A small amount of Zn nuclei was deposited on a copper grid. Grid was washed by ethanol and excess ethanol was blotted away with filter paper. And then, the copper grid with zinc nuclei was plunged into liquid nitrogen to avoid oxidation. The grid was transferred in nitrogen to perform TEM using a Tecnai G^2 20 transmission electron microscope (FEI Co.). The X-ray diffraction patterns (XRD) of Zn film were collected on a Rigaku D/max2550 diffractometer using Cu *Kα* radiation (40 kV, 200 mA, λ=0.154 nm), with a slit width of 0.25° and the 2θ ranged from 10° to 80°. The crystal size (*D*) was calculated from diffraction peak half-widths of (101) plane using Scherrer's equation. Scanning electron microscopy (SEM) was performed using a JEOL JSM-5600LV microscope at an accelerating voltage of 9 kV.

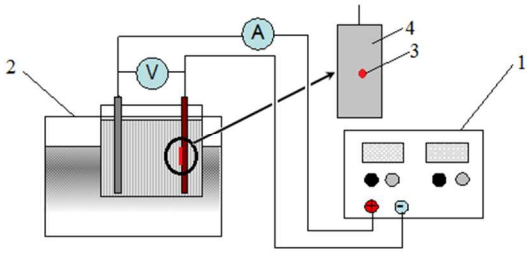

Fig.1. Schematic representation of zinc electrodeposition setup
1- DC stabilized power supply; 2-Thermostatic waterbath; 3- Copper grid; 4-Wrapped Ti- cathode

The electrochemical setup was a conventional three-electrode cell with titanium plate as work electrode of surface area of 1.0cm^2, a platinum plate of surface area of 1.0cm^2 as counter electrode and saturated calomel electrode as reference electrode. Work electrode was enclosed in epoxy resin and polished to mirror finish with 3μm abrasive paper, and then washed by acetone and alcohol. All potentials reported here were expressed with respect to the saturated calomel electrode(SCE). The electrochemical experiments were controlled using a Galvanostat CHI660C (CH Instrument, China) linked with a computer collecting the experimental data.

3 Results and discussion

3.1 XRD characterization of Zn deposits

Fig.2 illustrated the XRD patterns of Zn deposits from Zn(II)-NH_3-NH_4Cl-H_2O electrolyte (0.5 mol/L of Zn^{2+}, 5.0mol/L of NH_4Cl, and 1.8mol/L of $NH_3 \cdot H_2O$) with different gelatin content. The results illustrate that the peaks indexed as (002), (100), (101), (102), (103) and (110) appear in XRD patterns indicating that hexagonal Zn (ICDD# 65-3358, P63/mmc (194)) has formed. It is interesting that the intensity of (101) plane of zinc decrease and then increase with increase of gelatin concentration in electrolyte. A minimum intensity shows us when the gelatin concentration is 75mg/L. However, the variation of intensity of (110) reflection with the change of gelatin concentration is reverse order.

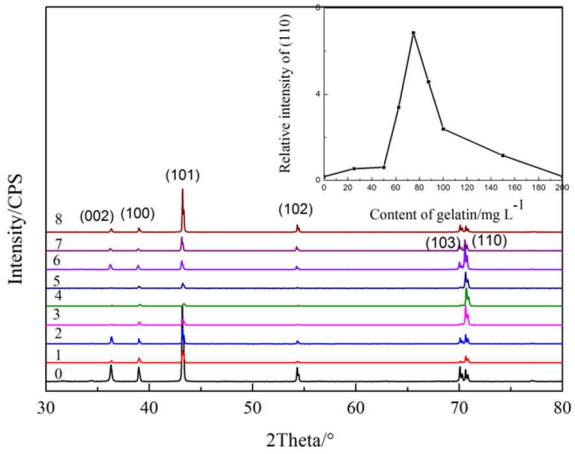

Fig.2. XRD patterns of deposited Zn from electrolyte and Lotgering factor of (110) plane (Inset) with different gelatin content 0-0mg/L, 1-25mg/L, 2-50mg/L, 3-62.5mg/L, 4-75mg/L, 5-87.5mg/L, 6-100mg/L , 7-150mg/L, 8-200mg/L

The change of the relative intensity of (110) plane to (101) plane of the electrodeposited Zn obtained from Zn(II)-NH_3-NH_4Cl-H_2O system with different content of gelatin was shown in inset of Fig.2. The results show us a maximum relative intensity when the content of gelatin in electrolyte is 75 mg/L. The higher is the diffraction peak, the greater is the oriented growth of zinc possibly.[25,26] Zinc crystal is hcp structure with 3 planes equivalent to (110) plane. Consequently, the gelatin is played a role of enhancing growth of {110} orientation, perpendicular *c*-axis orientation, when the gelatin concentration is 75 mg/L.

The degree of {110} orientation of Zn crystals as a function of content of the gelatin was evaluated from the intensity of the XRD peaks using following equations according to the Lotgering factor *f*:[27]

$$f = \frac{\rho - \rho_0}{1 - \rho_0}$$

and

$$\rho_0 = \frac{\sum I_0\{110\}}{\sum I_0(hkl)}$$

$$\rho = \frac{\sum I\{110\}}{\sum I(hkl)}$$

where I and I_0 are the relative intensities of each reflection peak of the (h k l) planes; ρ is the value calculated from the XRD data measured for our samples and ρ_0 is the value calculated from the standard XRD data (ICDD #65-3358). Commonly, Subscript 0 corresponds to a random sample. The f factor changes between 0 and 1. A large f value implies a highly textured material, since f = 0 for a random sample and f = 1 for a fully oriented material. This result is shown in Fig. 3.

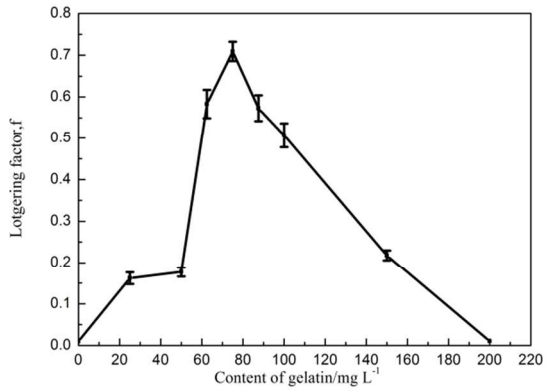

Fig.3 The degree of perpendicular c-axis orientation of Zn electrodeposition as a function of gelatin concentration

The Lotgering factor f increased up to 0.71 with increase in gelatin concentration in solution, and decreased down to 0.01 by subsequent increasing of gelatin concentration up to 200 mg/L. It was clear that zinc crystal tended to obvious orient due to effects of gelatin. The results were consistent with the tendency of relative intensities of XRD peaks. As stated above, another result could also be obtained that growth orientation of {101} plane became more and more prominent when gelatin concentration increased from 75 mg/L to 200 mg/L according intensity of XRD patterns.

3.2 TEM and HRTEM characterization of Zn nuclei on cathode

In order to further understanding the relationship between Zn crystal growth and concentration of additives in solution, zinc nuclei were deposited on a copper grid directly in Zn(II)-NH_3-NH_4Cl-H_2O system containing 25mg/L, 75mg/L and 150mg/L of gelatin and characterized using TEM and HRTEM, respectively (shown in Fig.4 and Fig.5). The results indicated that fibrous structure formed when gelatin concentration was 25 mg/L and the particle size was less than 30nm when gelatin concentration was 75mg/L. The preferable adsorption of gelatin on zinc nuclei occurred on the (110) plane and its equivalent planes. However, the zinc nuclei became fibrous structure when the gelatin content was far from 75mg/L in solution due to decrease in growth rate of {110} orientation of Zn nuclei.

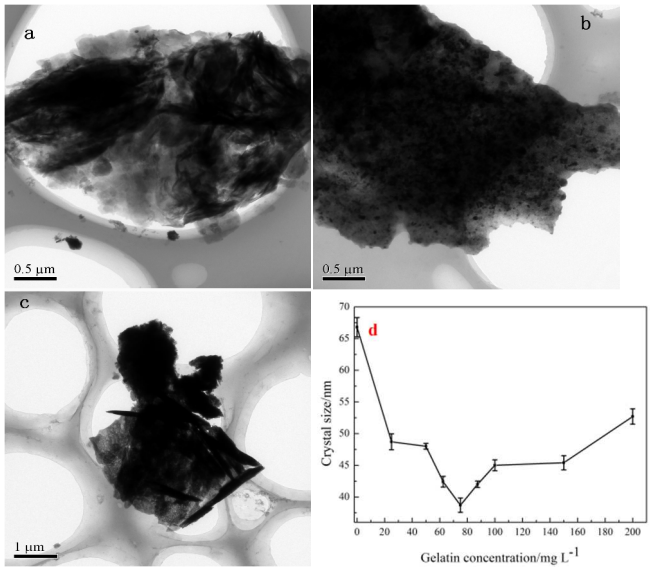

Fig.4 TEM images and crystal size distribution based on (101) reflection of zinc deposits on cathode
Gelatin concentrations: a-25mg/L, b-75mg/L, c-150mg/L, d-crystal size distribution based on (101) reflection.

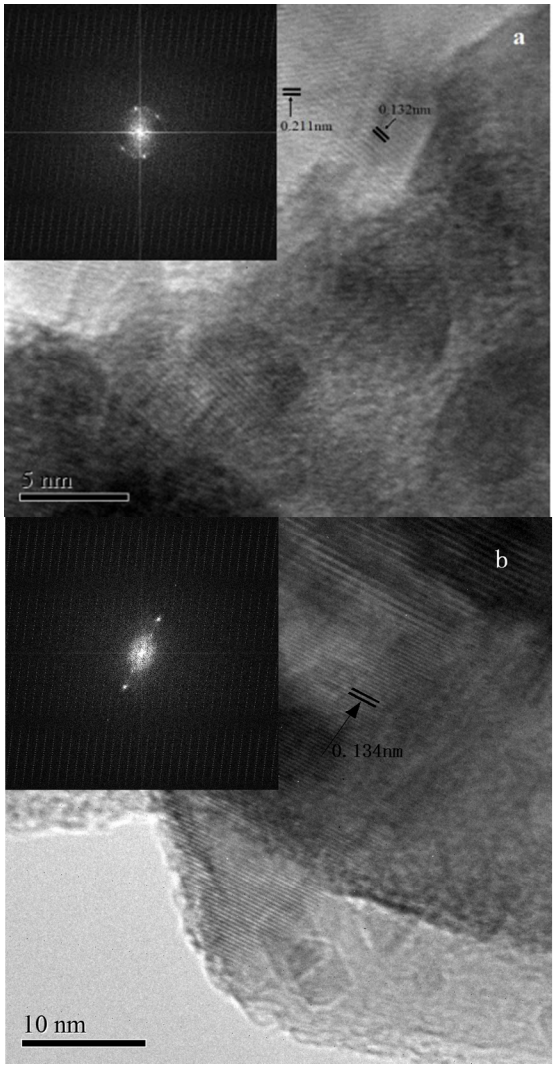

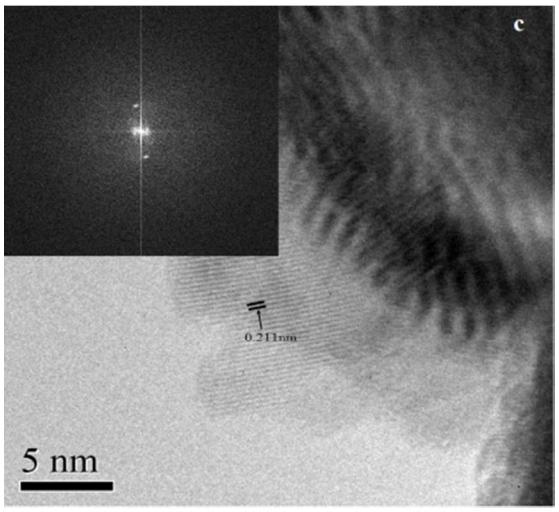

Fig.5 HRTEM images of zinc nuclei deposited on cathode (Insets are FFT images of the HRTEM)
Gelatin concentrations: a-25mg/L, b-75mg/L, c-150mg/L

Moreover, the crystallite sizes of Zn could be calculated based on the full width at half maximum of the (101) reflection from the following Scherrer's equation.[28]

$$D = K\lambda/\beta \cos\theta$$

where D is the crystallite size, λ (0.15406 nm) is the wavelength of characteristic X-rays, θ is the Bragg angle, K is the Scherrer constant, and β is the calibrated full width at half maximum of diffraction peaks. The variation of crystalline sizes on gelatin concentration is shown in Fig.4(d).

Gelatin is composed of the amino acids as collagen. The most important amino acids of collagen include arginnine, hydroxylysine, asparghinic acid, glutaminic acid, hydroxyproline, histydine, methionine, and so on, which have -NH_2 groups,-COOH groups, -NH group, and -SCH_3 group presented on the gelatin film surface, respectively. Additionally, there are peptide bonds in gelatin, the presence of the –NH–C=O groups also are on the gelatin film surface.[29] These groups were adsorbed selectively on the tip of fibrous zinc microcrystal and inhibit the random orientation of zinc crystal resulting in smaller size of particle when the gelatin concentration increases to 75 mg/L. However, with increase of gelatin concentration in electrolyte, adsorption of molecules of amino acids continued to occur on the other crystal plane when {110} planes were covered completely by amino acids of collagen at gelatin concentration of 75 mg/L. Consequently, orientation growth of {110} plane transited into random growth again, which caused increasing in crystal size based on (101) diffraction peak of Zn.

The HRTEM images exhibit the lattice spaces of 0.211nm and 0.132 nm(Fig. 5(a) and Fig.5(c)), and the lattices are attribute to (101) and (110) plane of zinc crystal, respectively. However, HRTEM images (Fig.5(b)) reveal the lattice spacing of 0.134nm, corresponding to that of (110) plane of Zn nanocrystals. There is a little shift to small angle. The FFT image illustrates the zinc nanocrystal is hexagonal structure typically (Shown insets to Fig.5(b)). The results were in agreement with those from XRD and further confirmed that the additives of gelatin could changed the growth orientation of Zn crystal.

3.3. SEM characterization of Zn deposits on cathode

The additives played most important role in formation of the compactness and smoothness of Zn deposits from the Zn(II)-NH_3-NH_4Cl electrolyte. When gelatin concentration is 75mg/L, a compact and smooth Zn sheet observes. Fig.6 shows that the SEM images of Zn deposits on cathode obtained at different gelatin concentration in solution containing 0.5 mol/L of Zn^{2+} and 5.0mol/L of NH_4Cl, 1.8mol/L of $NH_3 \cdot H_2O$. The results indicate that Zn deposits consist of grains. The microstructure of each grain consists in close crystal structure of flake Zn (Shown in inset of each SEM image in Fig.6). A close packed structure by Zn flakes in grains appears indicating that orientation growth is observed when the gelatin concentration is 75 mg/L(Fig.6(b)), contrariwise, it shows a random orientation. Some small cavities appear between crystal platelets. The change of size of Zn grains and quantities of cavities with gelatin concentration is consistent with that of crystal size based on (101) diffraction peak. The compactness and smoothness of Zn deposits on cathode depended on two aspects: firstly, the primary crystalline sizes of Zn nuclei dominated the sizes of secondary Zn grains. The smaller was primary crystal size, the more compact was the Zn deposits on cathode. Secondly, the intergranular pores and cavities in zinc grains played a significant role as the formation of compact electrodeposited Zn sheet. The quantities of cavity in Zn grain decreased the density of Zn sheet resulting in low compactness.

Combined the results of XRD characterization, the obvious growth orientation of Zn crystal based on (110) diffraction peak obtained from electrolyte with 75mg/L of gelatin concentration conduce to form intergranular pores and cavities in small quantities. A proper concentration of gelatin could change the growth rate of zinc crystal and decrease the porosity of zinc sheet on cathode. Consequently, the compact Zn electrodeposited sheet could be obtained in electrolyte with 75mg/L of gelatin.

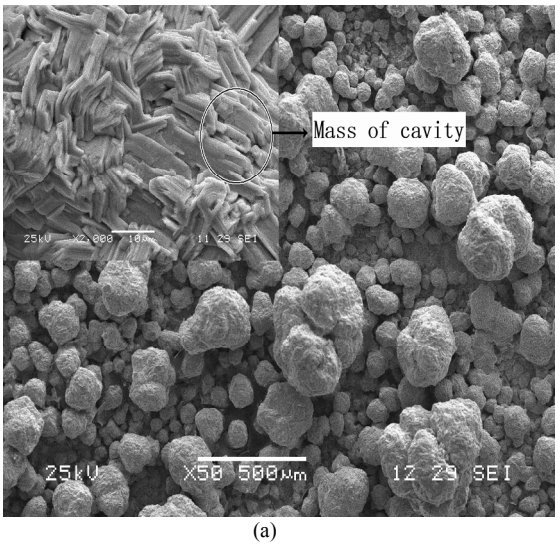

(a)

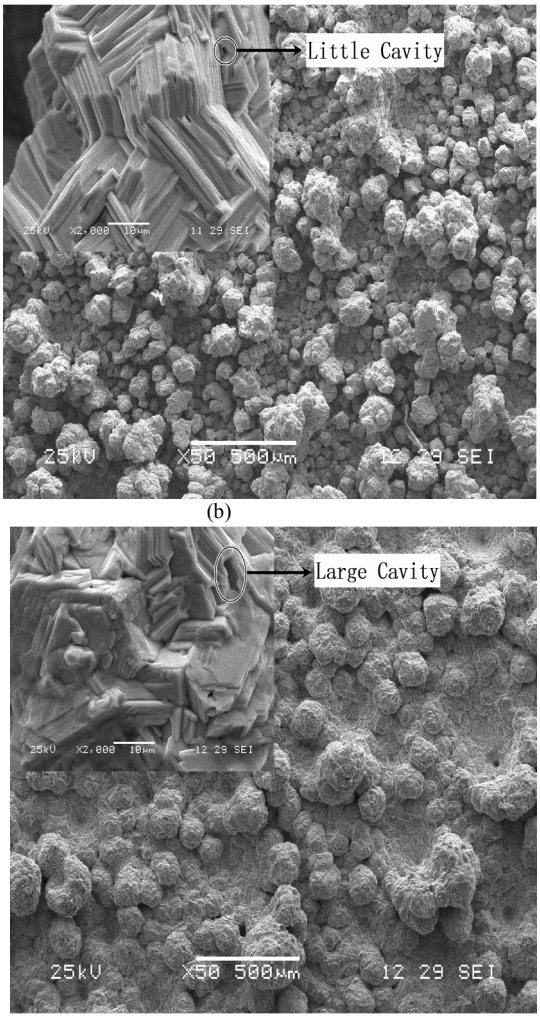

Fig.6 SEM images of zinc deposits on cathode from electrolyte with different gelatin concentration (Insets is high amplification of the SEM image)
Gelatin concentrations :a-25mg/L, b-75mg/L, c-100mg/L

3.4 Voltammetric study in the presence of gelatin

Cyclic voltammetry studies were performed within the potential range of -0.20 to -1.6V using a titanium electrode. The potential scan was initiated in the negative direction from the initial potential (-0.2 V) at a scan rate of 50mVs^{-1}. Fig.7 shows a typical voltammogram obtained from Zn(II)-NH_3-NH_4Cl electrolyte with different content of gelatin. The cathodic parts of the curves illustrate behavior characteristic of metal deposition occurring by nucleation. During the potential scan in the negative direction, it was necessary to impose an overpotential to initiate the formation of nuclei on the electrode surface. After nucleation began, a fast increase in cathodic current density was observed, resulting in peak Ic corresponding to the reduction of Zn(II) ions to Zn(0). The current density at peak changed with different gelatin content accompanying with a little shift to more negative potential, which minimum value of current density appeared at gelatin content of 75 mg/L in solution(Shown in inset (a) of Fig.7). The phenomena came from adsorption of gelatin on the surface of titanium crystal and then on the surface of zinc crystal as well. It blocks a fraction of the active sites at which the first reduction process occurs. These are consistency with results reported by Ballesteros et al[30] and above TEM results. On switching the potential scan at -1.6V and scanning in the positive direction, due to the difference in deposition and dissolution potentials, it provokes the formation of two crossovers between the positive and negative current traces at the crossover potential E_x, characteristic for nucleation processes.[31,32] The overpotential was defined as potential difference between crossover potential and reduction potential shown in inset (b) of Fig.7. The maximum overpotential of 0.01V was obtained when gelatin content was 75mg/L, which was more than 0.003V of overpotential in electrolyte added 150mg/L gelatin and 0.002V of overpotential in electrolyte added 25mg/L gelatin.

It was interesting that there were two anodic stripping peaks on positive scans without cathodic counterpart, namely -1.24V and -1.04V respectively. The current density at peak -1.04V became larger and larger with increase of the *f* factor of zinc crystal. It was reasonable herein that the anodic peak at -1.04V was assigned to dissociation of zinc crystal with {110} orientation and other anodic peak at -1.24V was corresponded to zinc crystal with random orientation. The difference of stripping potential resulted from corrosion inhibition of selective adsorption of gelatin on (110) plane through -NH_2 groups,-COOH groups, -NH group, and -SCH_3 group presented on the gelatin molecules.[29]

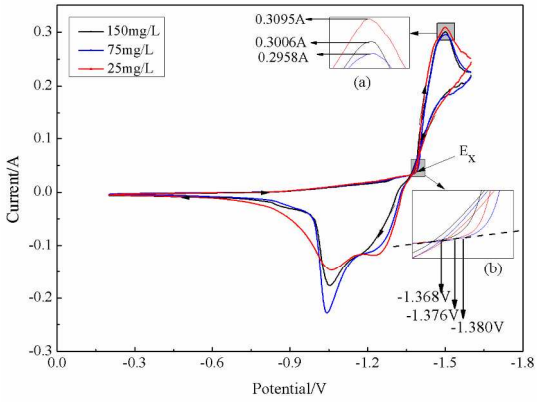

Fig.7. Voltammogram obtained on a titanium electrode in Zn(II)-NH_3-NH_4Cl solution with different gelatin content.

4. Conclusions

In summary, gelatin played a significant role of changing growth orientation from random to {110} preferable orientation with maximum Lotgering factor of 0.71 after gelatin addition of 75 mg/L because selective adsorption of gelatin on surface of zinc nuclei occurred during zinc electrodepositing in electrolyte of Zn(II)-NH_3-NH_4Cl-H_2O. Inhibition of random orientation resulted in absence of fibrous Zn nuclei in primary grain and decreased the porosity of electrodeposited-Zn film in presence of 75 mg/L of gelatin. The structure and morphologies of Zn nuclei were achieved using SEM, TEM and HRTEM. Cyclic voltammetric results showed us that increase of overpotential, negative shift of zinc nucleation potential and corrosion inhibition

of zinc crystal with {110} orientation were observed due to adsorption of gelatin on the surface of titanium plate and (110) plane.

Acknowledgements

This work was supported by the National Basic Research Program of China (2014CB643404) and the S&T Planning Project of Hunan Province (no. 2013GK3046).

Notes and references

[a] *School of metallurgy and Environment, Central South University, Changsha 410083 P.R.China*
E-mail: yangshcsu@163.com; zhimei_x@163.com; Tel:+86 18973385951;Fax:+86 731 22183465
[b] *School of Metallurgical Engineering, Hunan University of Technology, Zhuzhou 412007 P.R.China*

1 A.D. Zunkel, Fourth International Symposium on Recycling of Metals and Engineered Materials, Pittsburgh, Pennsylvania, U.S.A., 2000, 22-25, 227-236.
2 M. Olper, M. Maccagni, Fourth International Symposium on Recycling of Metals and Engineered Materials, Pittsburgh, Pennsylvania, U.S.A., October 2000,22-25, 379-396.
3 S.H. Yang, M.T. Tang, Y.F.Chen, C.B. Tang, J. He, Trans. Nonferrous. Met. Soc. China. 2004, 14, 626-629.
4 S.H.Yang, M.T. Tang, Trans. Nonferrous. Met. Soc. China. 2000,10, 830-833.
5 R.X. Wang, M.T. Tang, S.H.Yang, W.H. Zhang, C.B. Tang, J. He, J.G. Yang, J. Cent. South. Univ. Tech. 2008, 15, 679-683.
6 Z.Y. Ding, Q.Y.Chen, Z.L.Yin, K. Liu, Trans. Nonferrous. Met. Soc. China. 2013,23, 832-840.
7 J.Vazquez-Arenas, F. Sosa-Rodriguez, I. Lazaroc, R.Cruz, Electrochim.Acta. 2012,79,109-116.
8 K.Hernández, J. Vazquez-Arenas, R. Cruz, ECS Transactions, 2008,15,161-169.
9 A.M. Lafront, W.Zhang, E.Ghali, G.Houlachi, Can. Metall. Quart. 2009,48, 337-345.
10 S.E.Afifi, A.R. Ebaid, M.M.Hegazy, A.K. Barakat, , JOM. 1992,44,32-34.
11 T.Ohgai, H. Fukushima, N. Baba, T. Akiyama, Proceedings of the TMS Fall Extraction and Processing Conference, LEAD-ZINC ,2000.855-863.
12 D.S. Baik, D.J. Fray, J. Appl. Electrochem. 2001,31,1141-1147.
13 A.E. Saba, A.E. Elsherief, Hydrometallurgy 2000,54,91-106.
14 R.L.Yu, Q.M. Liu, G.Z. Qiu, Z. Fang, J.X.Tan, P.Yang, Trans. Nonferrous. Met.Soc.China. 2008,18, 1280-1284.
15 T.Mukongo, K.Maweja, B.W.Ngalu, I.Mutombo, K.Tshilombo, Hydrometallurgy, 2009, 97, 53-60.
16 B.C.Tripathy, S.C. Das, J. Appl. Electrochem. 1998,28, 915-920.
17 D.J.Mackinnon, J.M.Brannen, J. Appl. Electrochem. 1977,7, 451-459.
18 G.Trejo, H.Ruiz, R.Ortega Borges, Y.Meas, J.Appl.Electrochem. 2001,31,685-692.
19 L.E.Morón, A.Méndez, F.Castañeda, J.G.Flores, L.Ortiz-Frade, Y.Meas, G.Trejo, Surf.Coat.Tech. 2011,205,4985-4992.
20 D.Dhak, E.Asselin, S.Di Carlo, A. Alfantazi, ECS Trans. 2010, 28, 267-280.
21 D.J.Mackinnon, R.M.Morrison, J.E.Moulend, P.E.Warren, J. Appl. Electrochem. 1991,21, 213-220.
22 A.E.Alvarez, D.R.Salinas, J. Electroanal. Chem. 2004,566, 393-400.
23 L.M.A.Monzon, L.Klodt, J.M.D.Coey, J. Phys. Chem. C. 2012, 116, 18308−18317.
24 J.X.Yu, L.Wang, L.Su, X.P.Ai, H.X.Yang, J. Electrochem.Soc. 2003, 50, C19-C23.
25 D.J.Mackinnon, J.M.Brannen, R.M.Morrison, J. Appl. Electrochem. 1988,18, 252-256.
26 X.L. Xia, I. Zhitomirsky, J.R. McDermid, J.Mater.Processing.Tech. 2009, 2632-2640.
27 F.K.Lotgering, J. Inorg. Nucl. Chem. 1959, 9,113-123.
28 H. Schmidta, E.R. Fotsinga, G. Borchardta, R. Chassagnonb, S. Chevalierb, M. Brunsc, Appl. Surf. Sci., 2005, 252, 1460.
29 T.Białopiotrowicz, B.Jańczuk, Langmuir. 2002,18, 9462-9468.
30 J.C.Ballesteros, P.Díaz-Arista, Y.Meas, R.Ortega, G.Trejo, Electrochim. Acta. 2007,52, 3686-3696.
31 G. Gunawardena, G. Hills, I. Montenegro, J. Electroanal. Chem. 1985,184, 357-369.
32 D. Grujicic, B. Pesic, Electrochim. Acta. 2002,47, 2901-2912.